Performance of ferrierite promoted with tungsten or boron species during the linear butene skeletal isomerization

Alejandro Astudillo, Darío Fauda, Carlos Querini and Raúl Comelli[*]

Instituto de Investigaciones en Catálisis y Petroquímica - INCAPE (FIQ-UNL, CONICET). Santiago del Estero 2654, S3000AOJ - Santa Fe, Argentina

ABSTRACT

Ammonium and potassium ferrierite were modified with tungsten or boron species using incipient wetness and wet impregnation or ion exchange. Catalytic behavior in the linear butene skeletal isomerization was measured at 300 and 450ºC, atmospheric pressure and 0.15 atm 1-butene partial pressure. Catalysts having strong acid sites reach at 300ºC and a short time practically the same high butene conversion with low isobutene selectivity. Those acid sites favor undesirable side reactions. Conversion decreases at long time. At a short time, tungsten exchanged on potassium-ferrierite produces two times the ferrierite's isobutene yield. At long time, boron impregnated on ferrierite reaches the largest isobutene production. At 450ºC, the high conversion is maintained even at long time. At this temperature, tungsten impregnated on potassium-ferrierite, sample without strong acid sites, produces practically the same isobutene yield of ferrierite, although its conversion is only a half of the ferrierite one. By considering by-product distributions, dimerization and oligomerization reactions take place. Carbonaceous deposits were characterized by temperature-programmed oxidation and FTIR. The acid strength of active sites influences the coke amount. Independent of temperature, deposit formed on samples with strong acid sites is between 6.0 and 7.4%. The smallest amount (1.0%) is formed on tungsten impregnated potassium-ferrierite, which only displays the low-temperature combustion peak after reaction at 300ºC. Reaction temperature and type of acid sites affect the nature of carbonaceous deposit. Both olefinic species and aromatics rings appear in the deposit formed at 300ºC; at 450ºC, aromatic coke increases. Isobutene dimeric species play a role in coke formation.

1. INTRODUCTION

Changes in the balances of petrochemical plants generate demand of some captive compounds, which are used in other synthesis processes. In this way, the skeletal isomerization of linear butenes is an alternative route for the production of isobutene, which is used for the methyl tert-butyl ether synthesis and for the poliisobutene production. That skeletal isomerization reaction takes place on acid catalysts and demands a stronger acidity than the double bond isomerization. However, a strong acidity also favors undesirable side reactions such as dimerization-oligomerization, cracking, disproportion, and hydrogen transfer. Then, an ideal skeletal isomerization catalyst should have an adequate acidity in order to

*Corresponding author
rcomelli@fiqus.unl.edu.ar

selectively promote the isomerization reaction but not the undesirable side ones.

Ferrierite, a zeolite with a bidimensional pore structure of 10-membered rings (4.2 x 5.4 Å) intersected by 8-membered rings (3.5 x 4.8 Å), shows one of the best catalytic performances in the skeletal isomerization of linear butenes [1]. Its characteristic behavior is a high activity with low isobutene selectivity at a short time-on-stream (TOS); then, conversion decreases and selectivity increases after some minutes under reaction conditions [1,2]. Catalytic improvement of both potassium and ammonium ferrierite by tungsten species impregnation, following the incipient wetness technique and using both tungstic acid and ammonium metatungstate as tungsten precursors, was previously reported [3]. The presence of tungsten species on ferrierite improves the catalytic behavior without modifying the acidity profiles corresponding to the unpromoted materials [4]. Results of catalytic studies on ZSM-5 and ZSM-11 synthesized with different contents of aluminum and boron suggested that there are synergistic effects between framework boron and aluminum to enhance the butene skeletal isomerization activity [5]. These authors also concluded that incorporating boron into the framework can weaken the acidity of aluminum zeolites. The boron atom is smaller than aluminum one and occurs preferably in the trigonal coordination [6].

In order to characterize exchange sites in the ferrierite framework, the location of Cu cations in the dehydrated copper ion exchanged ferrierite [7] and Ni ion sites in hydrated and dehydrated forms of nickel-exchanged ferrierite [8] were analyzed. Lithium and cesium-exchanged ferrierite were evaluated to investigate the effect of the presence of acid sites on the external surface, the acid site density and the space around the site over the isobutene selectivity [9]. More recently, the catalytic properties of ferrierite exchanged with alkaline earth metals in the linear butene skeletal isomerization [10] and the selective formation of alkenes through the n-heptane cracking on Ca-exchanged ferrierite [11], were reported.

Deactivation of acid zeolites used in hydrocarbon transformations is mainly due to the formation of carbonaceous deposit inside the pores. The pore structure, the acidity and the operating conditions influence the coking rate and the deactivating effect of coke molecules [12]. The characteristic catalytic behavior of ferrierite has been related to the carbonaceous deposit formation [2, 13], the type of acid sites [14], the space around the acid sites [9], and the acid sites density [15]. The reaction mechanism of linear butene skeletal isomerization on ferrierite remains under discussion. Nevertheless, the fresh material is accepted as non-selective, whereas the aged one is considered selective. The carbonaceous deposit formed on ferrierite during the butene skeletal isomerization reaches levels between 7 and 9% [2, 13, 16-18]. We have characterized the carbonaceous deposit formed on ferrierite during this skeletal isomerization; it has both olefinic and aromatic nature and the proportion strongly depends on the operating conditions [19]. An exhaustive analysis of deactivation of solid acid catalysts during the linear butene skeletal isomerization, including a reaction scheme of the formation of carbonaceous deposits, the possible reactions occurring during the transformation as a function of TOS, and the locations of the active sites, has been published [20].

Topics related to ferrierite deactivation have previously concentrated the main interest, especially in order to understand the isobutene selectivity improvement with TOS. Nevertheless, an ideal catalyst gives an adequate activity with high selectivity and yield starting from a short time and maintaining the performance with TOS. Then, the promotion of ferrierite with species in order to reduce the high activity with low selectively at a short TOS and to improve the catalyst stability is an interesting subject to investigate.

Linear butene isomerization over ferrierite modified with tungsten and boron species is studied in this paper. Catalysts are prepared either by both incipient wetness and wet impregnation or by ion exchange, using

potassium and ammonium ferrierite as starting materials. The catalytic behavior of samples is evaluated at 300 and 450ºC and at atmospheric pressure. In order to study deactivation processes, the carbonaceous deposit formed during the butene reaction is characterized by temperature-programmed oxidation (TPO) and Fourier transformed infrared spectrometry (FTIR).

2. EXPERIMENTAL

2.1. Catalyst preparation

Ammonium and potassium ferrierites, identified as NH_4-FER and K-FER, respectively, were provided by TOSOH, Japan (samples HSZ-720NHA and HSZ-720KOA, respectively). The SiO_2/Al_2O_3 molar ratio was 17.8. NH_4-FER has Na_2O and K_2O concentrations below 0.05 and 0.10%, respectively. The crystalline structure was characterized by X-ray diffraction, being the spectrum range $3 < 2\theta < 60º$ [3].

Catalysts were prepared by incipient-wetness impregnation (IWI), wet impregnation (WI), and ion-exchange (IE). Tungstic acid (Sigma), tungsten(VI)-dichloride-dioxide (Aldrich), and boric acid (Cicarelli) were used as tungsten (W) and boron (B) precursors, respectively. Solutions with the desired concentration were prepared. After the incipient-wetness impregnation, samples were maintained 4 h at room temperature and then dried overnight in an oven at 110°C. NH_4-FER and K-FER were used as starting materials for ion exchange. Typical conditions for wet impregnation and ion exchange were: 1 g of catalyst for 11 ml solution as solid-liquid ratio, 60°C, pH between 4 and 5, and continuous stirring during 6 h. Then, the materials were filtered, washed with deionized water until free of chloride ions, and dried overnight in an oven at 110°C; more details were previously reported [21]. Table 1 shows sample identification, starting material, preparation technique, precursor used, and the loading on the final material.

2.2. Catalyst characterization

The surface species reducibility was determined by temperature-programmed reduction (TPR) using an Ohkura TP 2002S equipped with a thermal conductivity detector. Samples were pretreated in-situ in a nitrogen (60 ml min^{-1}) plus air (50 ml min^{-1}) stream, heating at 9.6°C min^{-1} and holding 60 min at 600°C. Then, samples were cooled to room temperature in an argon stream, and finally heated at 10°C min^{-1} up to 950°C in a 1.8% hydrogen in argon stream.

Ammonia temperature-programmed desorption (NH_3-TPD) measurements were carried out to characterize the total acidity and the acid strength distribution of the catalysts. Samples

Table 1. Sample identification, starting material, preparation technique, precursor used, and loading on the end material.

Sample identification	Starting material	Preparation technique	Precursor	Loading (wt.%)
W/FER	NH_4-FER	IWI [a]	Tungstic acid	0.8
W-FER	NH_4-FER	IE [b]	Tungsten-(VI)-dichloride-dioxide	n.d.
W/K-FER	K-FER	IWI	Tungstic acid	3.5
W-K-FER	K-FER	IE	Tungsten-(VI)-dichloride-dioxide	4.8
B/FER	NH_4-FER	IWI	Boric acid	0.8
B-FER	NH_4-FER	WI [c]	Boric acid	n.d.
B/K-FER	K-FER	IWI	Boric acid	0.8

(a): incipient wetness impregnation; (b): ion exchange; (c): wet impregnation

were pretreated in situ under the same conditions mentioned above. Then, samples were cooled in a nitrogen stream. Ammonia was fed through a sample valve over the bed at 100°C, followed by a purge with nitrogen at 200°C during 120 min. Finally, temperature was raised at 10°C min^{-1} in a nitrogen stream. The ammonia desorption was continuously measured using a thermal conductivity detector.

2.2. Catalytic behavior

The catalytic behavior during the 1-butene reaction was measured in a continuous down-flow, fixed-bed quartz tubular reactor operated at atmospheric pressure, using 500 mg of catalyst sieved to 35-80 mesh. All samples were pretreated heating up to 600°C, and keeping this temperature for 30 min; then, they were cooled to the reaction temperature in a nitrogen stream. After this pretreatment, NH$_4$-FER was transformed into the protonic form, being identified as H-FER. For reaction, a pure 1-butene stream was co-fed with nitrogen at 0.15 atm 1-butene partial pressure. Reaction temperatures were 300 and 450°C.

The reactant and reaction products were analyzed by on-line gas chromatography, using a 30 m long, 0.54 mm o.d. GS-Alumina (J&W) megabore column, operated as follows: 5 min at 100°C, then heating at a rate of 10°C min^{-1} up to 160°C, keeping this temperature for 60 min. From these data, catalytic activity, isobutene yield, and by-product distribution were calculated on a carbon basis. The catalytic activity is expressed as linear butene conversion, grouping together the three linear butene isomers. It is based on the fact that, under reaction conditions, the 1- to 2-butene isomerization quickly reaches the equilibrium via double-bond migration.

2.3. Characterization of carbonaceous deposits

The carbonaceous deposit formed on catalysts during the butene reaction was characterized by TPO. This analysis was performed in an apparatus designed to improve both sensitivity and resolution [22]. Combustion products were completely converted to methane on a nickel catalyst, methane being continuously analyzed by a flame ionization detector. Experiments were carried out using a 6% oxygen in nitrogen stream (20 ml min^{-1}), heating 12°C min^{-1}. The sample weight was about 0.01 g. Calibration was periodically checked to verify the total conversion of both carbon monoxide and carbon dioxide into methane.

The carbonaceous deposit was also characterized by FTIR, using a SHIMADZU 8101M spectrometer. Coked samples were powdered and diluted to 2% in potassium bromide (Merck). Then, fine discs were prepared and placed into a cell designed for this characterization. Some measurements at room temperature were made injecting butene into the cell, through a sampling valve. These experiments were made with and without catalyst under vacuum.

3. RESULTS

3.1. Catalyst characterization

Previous characterization of NH$_4$-FER and K-FER by TPR did not show reduction peaks [4]. Tungsten-impregnated samples displayed reduction peaks associated with tungsten species; profiles depend on the impregnated ferrierite form and on the tungsten loading [21]. The W/FER corresponding profile showed two overlapped peaks with maxima centered at about 620 and 740°C, respectively. The larger the tungsten loading on K-FER, the higher the reduction peaks but centered at similar temperatures; the largest peak displays its maximum at higher temperature. The presence of more than one peak would indicate that reduction can take place in steps, even though the relationship between areas under peaks does not allow us to consider the $W^{6+} => W^{4+} => W^0$ sequence. Tungsten-exchanged samples do not practically show any reduction peak, what indicates that tungsten has been incorporated into the zeolite framework. B/FER samples did not display peak while the B-FER showed the corresponding ones. It allows us to consider that after pretreatment, the B species do not remain on the surface on

samples prepared by incipient wetness impregnation while those species are present on samples prepared by wet impregnation.

NH$_3$-TPD characterization showed that W impregnation on both H-FER and K-FER does not modify the total acidity neither the distribution of non-impregnated corresponding materials [4]. Figure 1 displays characteristic
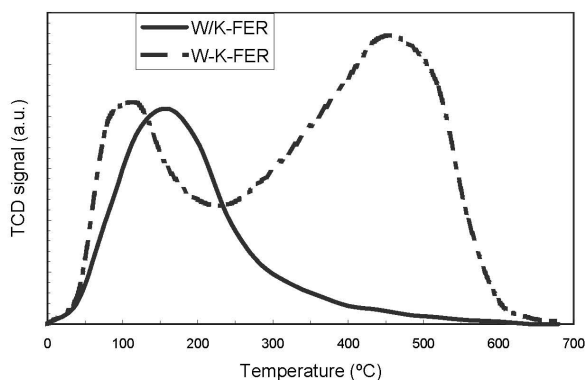

**Fig. 1.** NH$_3$-TPD profiles of representative samples.

profiles. Tungsten-impregnated on K-FER only presents the low temperature desorption peak, similar to the K-FER profile. W exchanged on K-FER displays both desorption peaks, changing the K-FER profile. The presence of B on H-FER reduces both desorption peaks.

3.2. Catalytic performance

Figures 2-a and 2-b present the linear butene conversion and the isobutene yield, respectively, for catalysts at 300 and 450ºC after 5 and 120 min of operation. Different behaviors can be observed during reaction at 300°C. H-FER reaches a high conversion after 5 min of reaction, decreasing it strongly at long TOS; the isobutene yield diminishes slightly with TOS. W/FER shows practically the same conversion compared to H-FER, while the isobutene yield remains constant with TOS and slightly larger than that corresponding to the unpromoted material. W-FER displays the same behavior at 5 min, with better conversion and isobutene production at long TOS as compared to W/FER. Tungsten impregnated on K-FER, promotes both activity and isobutene yield referred to
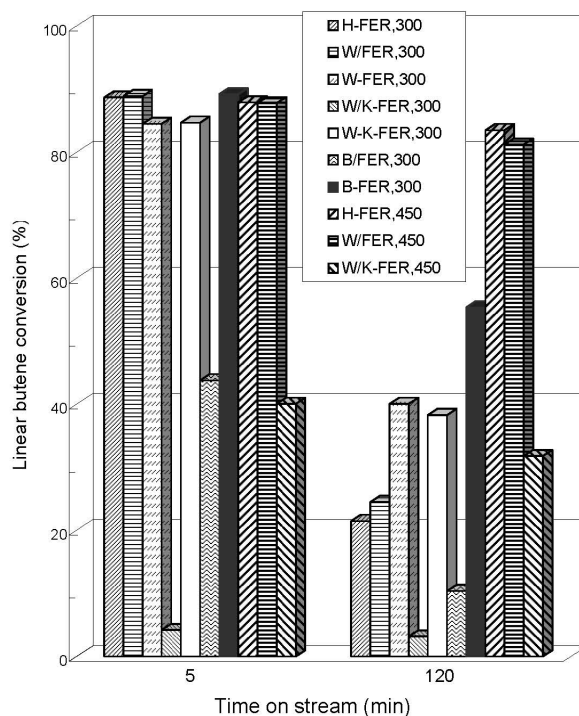
Fig. 2-a
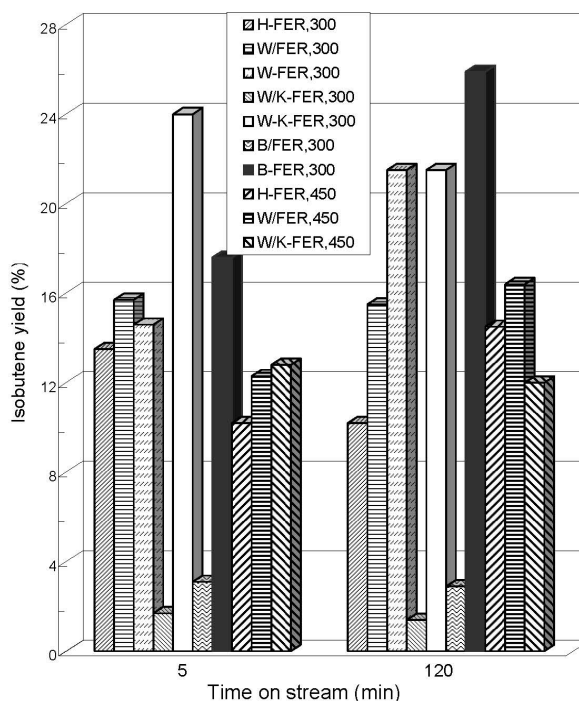
Fig. 2-b

Fig. 2. Linear butene conversion (a) and isobutene yield (b) at 5 and 120 min on stream during the 1-butene reaction on different catalysts at 300 and 450ºC (temperature indicated after sample identification and expressed in degree centigrade).

the non-impregnated material that is inactive [3]. Tungsten-exchanged K-FER shows the same behavior than W-FER, reaching the largest isobutene yield at 5 min. B/FER reaches approximately 40% butene conversion after 5 min while the isobutene yield is lower than 3%. B-FER displays a similar qualitative behavior than W/FER but improving the performance at long TOS, reaching the largest isobutene production. B/K-FER results inactive for the butene skeletal isomerization.

During reaction at 450°C, H-FER and W/FER maintain a high conversion even at long TOS, while at this time the isobutene yield increases. Working with W/K-FER, both linear butene conversion and isobutene yield grow practically one order of magnitude referred to the levels obtained at 300°C; conversion slightly decreases with TOS while the isobutene yield remains practically constant. Comparing with W/FER, the linear butene conversion obtained with W/K-FER is practically 50% lower but the isobutene yield is similar, improving the isobutene selectivity.

Figures 3-a and 3-b display the by-product distribution for selected samples at 5 and 120 min of operation, respectively. Methane, ethane and isobutane are produced only in very small amounts on all samples. At long TOS, propene and the C_5^+ fraction are the main by-products. Ethene, propane and linear butane appear on some samples. The presence of tungsten species modifies the pattern of by-product distribution referred to the H-FER corresponding one. The ethene+propane+propene fraction is larger than the C_5^+ one, being propene the main by-product. W/K-FER displays the most stable behavior with TOS. C_5 and C_6 alkenes are the main compounds present in the C_5^+ fraction. B-FER displays a by-product distribution similar to the H-FER one.

3.3. Characterization of carbonaceous deposits

Table 2 shows the amount of carbonaceous deposit formed on catalysts at 300 and 450°C after 200 min on stream. Independent of the reaction temperature, the deposits formed on H-FER, W/FER, W-FER, and W-K-FER reach levels between 6.0% and 7.4%. All these catalysts show a similar behavior regarding the amount of coke deposited. W/K-FER samples present a very different behavior even at 450°C, the amount of carbonaceous deposit is significantly smaller, lower than 1.5%. B/FER presents an intermediate behavior, being carbonaceous deposit 4.5% after reaction at 300°C.

Table 2 also displays the temperature of the maximum of combustion peaks in the TPO profiles. After reaction at 300°C, H-FER, W/FER, W-FER, W-K-FER, and B/FER present two well-defined combustion peaks centered at 325-345°C and 640-660°C, respectively, and a smooth one between them. W/K-FER shows a different behavior, the only combustion peak appears centered at 345°C. After reaction at 450°C, all the former samples present only the high-temperature combustion peak. Figure 4 shows TPO profiles of selected samples in order to illustrate results presented in Table 2.

Table 3 presents FTIR characterization of carbonaceous deposits on representative samples. After reaction at 300°C, H-FER, W/FER, W-FER, and W-K-FER, all catalysts having strong acid sites, present strong bands centered at 1140 cm^{-1} assigned to olefinic species, and at 1512 cm^{-1} related to aromatics; other weak and very weak bands at 1240, 1630, 1340, 1425, 2890, and 2960 cm^{-1} also appear. W/K-FER which have not strong acid sites, shows the main bands centered at 1130 and 1628 cm^{-1}, both assigned to butene species; two important differences with the previous catalysts are that the 1512 cm^{-1} band is very weak and the 1335 cm^{-1} one, associated to isobutene dimeric species, does not appear. B/FER displays a qualitative behavior similar to W/K-FER. After reaction at 450°C, the 1470 cm^{-1} aromatic corresponding band does not appear but a new band at 1590 cm^{-1} assigned to aromatic and polyaromatic species is observed.

In the OH region, samples display a medium band centered at 3640 cm^{-1}, a weak one centered at 3447-3500 cm^{-1}, and another small one at 3750 cm^{-1}. The intensity of the 3640 cm^{-1} band decreases for coked samples

Fig. 3-a
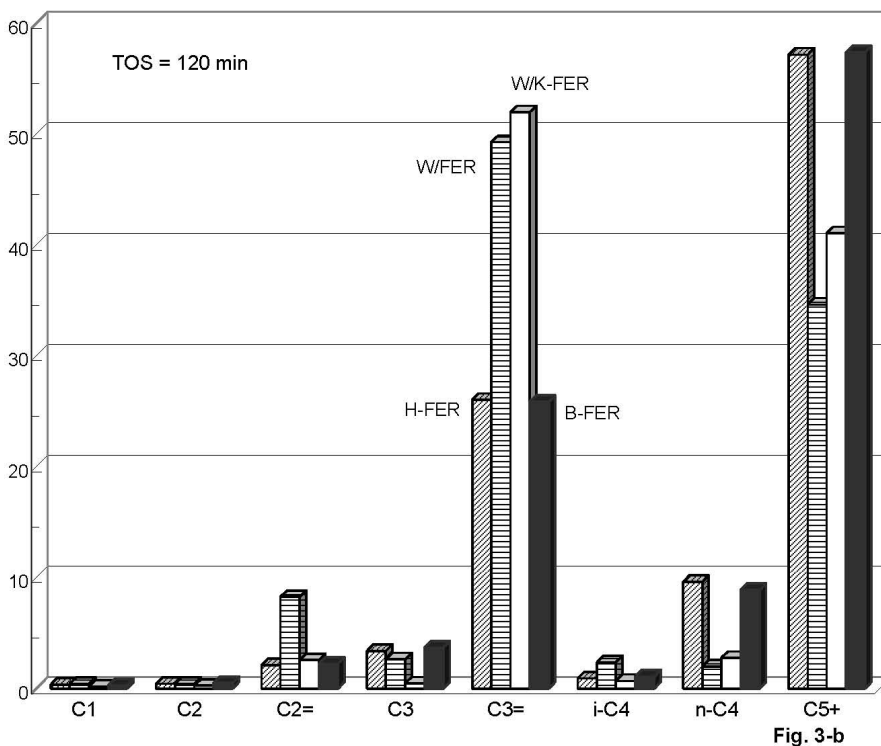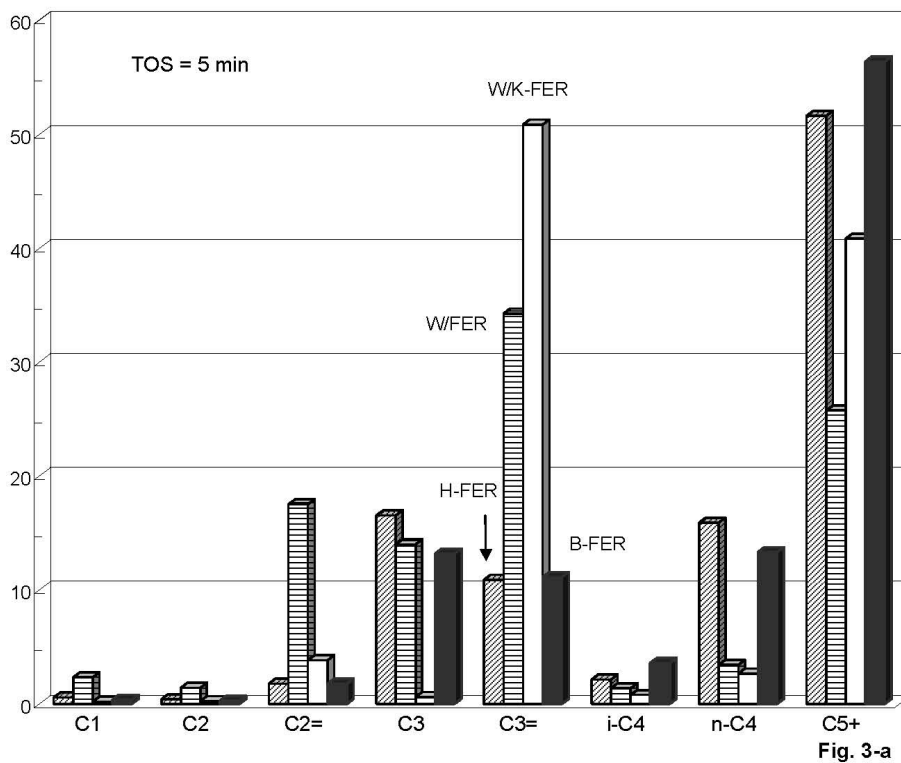
Fig. 3-b

Fig. 3. By-product distribution in the 1-butene reaction on representative samples at 5 min (a) and 120 min (b). Reaction at 300°C, atmospheric pressure, and 0.15 atm 1-butene partial pressure.

Table 2: Carbonaceous deposit and temperature of the maximum of combustion peaks in the TPO profiles for catalysts after the 1-butene reaction at 300 and 450ºC.

Sample	T (°C)	Carbon content (C %)	Temperature of the maximum of combustion peaks (°C)		
H-FER	300	7,0	340 *l*	430 *s*	650 *m*
W/FER	300	6,0	325 *l*	450 *s*	660 *m*
W-FER	300	6,6	335 *l*	440 *s*	640 *m*
W/K-FER	300	1,0	345		
W-K-FER	300	6,2	329 *l*	425 *s*	645 *m*
B/FER	300	4,5	335 *l*	450 *vs*	655 *m*
H-FER	450	7,4			667
W/FER	450	7,2			667
W/K-FER	450	1,5			588
B/FER	450	4,9			625

l:large, m:medium, s:small, vs: very small.
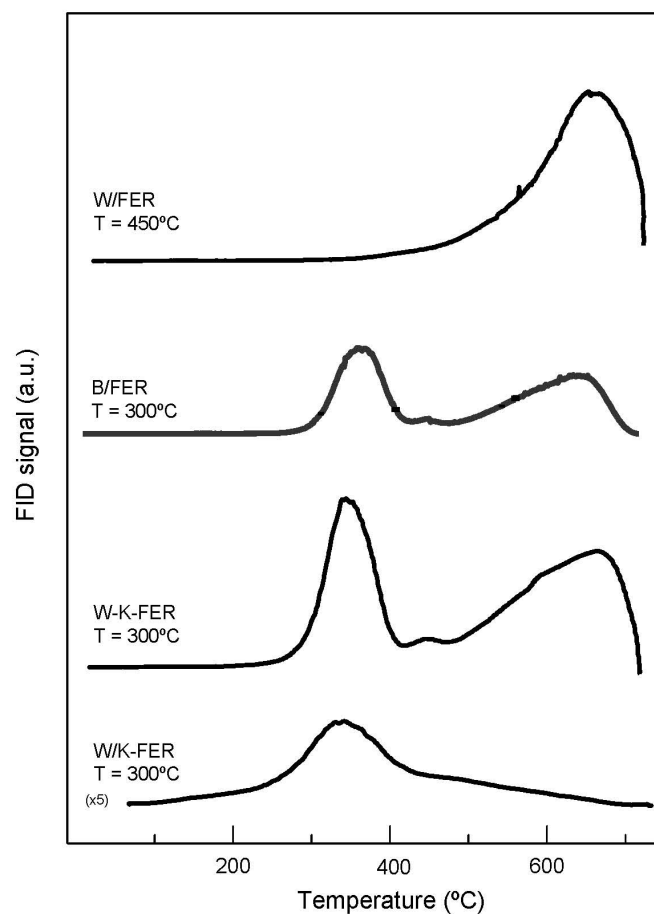
Fig. 4. TPO profiles of representative samples after the 1-butene reaction at 300 and 450°C.

Table 3: Bands (wavenumber values in cm^{-1}) observed in the 850-4000 cm^{-1} region of IR spectra on representative samples and their assignments.

H-FER (a)	W/FER (b)	W/K-FER (b)	B/FER (b)	W-FER (c)	B/FER (c)	Assignment
1020 s						
	1035vw	1035vw				1036/1045: νCC / CH$_3$ linear butene / i-C$_4^=$ bond π
	1140s	1130s	1077s	1078s	1078s	1110: linear butenes
1225vs						
	1240w	1240w	1233m	1240w	1240w	1240: wagging CH$_2$ long chain paraffins
	1340vw					1336: wagging CH$_2$ / i-C$_4^=$ dimeric
	1385vw					1385: aromatics-polyaromatics / δ CH$_3$
		1390vw	1398m		1400w	1390: olefinic species
	1425vw			1423vw		1420/1430: linear butenes / δ=CH$_2$ vinyl
	1460vw	1470vw				1450/1463: aromatic skeletal ring breathing / δ CH$_3$
	1512s	1512vw	1517w		1517w	1513/1524: γ C=C aromatics
			1590s			1590: aromatics-polyaromatics
1640m						
	1630w	1628m	1634m	1625w	1634m	1630/1625: iC$_4^=$ bond π / olefinic species
1640vs						
	2890vw	2890vw	2931w	2931vw	2937vw	2865/2925: saturated CH stretching
	2960w	2960w				2960: saturated CH / polyolefins + aromatics
		2990w			2987vw	2970/2990: saturated CH / stretching CH / olefinic species
3500w	3500w	3500w	3447w	3447w	3496m	3460: O..H-O-Si groups
3640m	3640m	3640m	3650w	3633m	3645m	3609/3640: OH associated to Si-Al ions / OH in supercage
3750vw	3750vw	3750vw		3750vw		

(a): only calcined sample.   (b): reaction temperature 300ºC.   (c): reaction temperature 450ºC.
vs: very strong; s: strong; m:medium; w: weak; vw: very weak.

and the 3750 cm^{-1} one remains practically constant [19]. On boralites, the 3460 cm^{-1} band was attributed to O···H-O-Si groups forming the hydrogen bond [23].

In order to carryout in-situ FTIR characterization, butene was injected into the cell at room temperature. In the absence of catalyst, butene displays intense bands at

915, 1002, 1464, 1630, and 2982 cm^{-1}. In the presence of catalyst and making vacuum after injection, the bands corresponding to the alkene are not detected, indicating the butene is not adsorbed under these conditions. Preliminary results injecting butene at 150 and 200°C on H-FER, W/FER, and B/FER display the 1512 cm^{-1} band as the first one formed.

4. DISCUSSION

4.1. Catalytic performance

The conversion of linear butenes does not occur at 100°C and reaches a low level during reaction at 200°C, being the isobutene yield negligible [23]. At 300°C, the skeletal isomerization of linear butenes takes place and the characteristic behavior of H-FER is observed: a high conversion with low isobutene selectivity at a short TOS, and lower conversion and higher isobutene selectivity at long TOS [1, 2]. Then, isobutene is produced above 300°C. The catalytic performance of the materials during the butene reaction can be affected by the environment of the acid active sites and their density [9, 15]. The high activity after 5 min of reaction with H-FER and W/FER has been previously related to the strong acid sites present on the surface of these materials [25]. These sites, which correspond to the high temperature peak in the NH$_3$-TPD profile, dominate the catalytic behavior. According to our results, it is also valid to W-FER, W-K-FER, and B-FER. W-K-FER prepared by IE presents strong acid sites, which are formed during catalyst preparation. W/K-FER prepared by IWI has not strong acid sites on the surface explaining the lower activity reached at a short TOS, which is practically constant with TOS. The high initial activity neither is observed when reaction takes place on B/FER; then, the impregnation of boron species by IWI affects the acid sites present on the surface. It was reported that Lewis acid sites on H-FER enhance oligomerization and cracking reactions [26]. These side reactions have been suppressed by removing the non-selective acid sites using acid treatment [27, 28]. Baeck *et al.* [29] studied the effect of boron on the acidic properties of Mg-ZSM-22 by impregnating with boric acid. It was found that boron mainly poisoned the strong acid sites, which resulted in a decrease in side reactions and an increase in the isobutene selectivity. Our results can be partially interpreted with the findings of Baeck *et al.* [29], because the isobutene yield is also diminished. Then, it allows us to consider the preparation technique has influence over the catalytic performance of materials.

When reaction takes place at 450°C, the high initial catalytic activity remains practically constant with TOS for each material, displaying a good stability. Nevertheless, the isobutene production is thermodynamically unfavored by increasing the reaction temperature. Materials having strong acid sites display a low isobutene selectivity but both W/K-FER and B/FER improve the isobutene yield.

The catalytic behavior can be also affected by the steric restriction imposed by the carbonaceous deposit formed inside the pores [2, 15]. The beneficial and harmful effects of carbonaceous deposits over the isobutene selectivity during the linear butene reaction were reported [20]. At long TOS at 300°C, the conversion is around 50% of the initial activity with all the catalysts. Coke deposition is the reason of this activity loss. However, at 450°C the activity loss is much lower, even though the total amount of coke is almost identical. Therefore, the coke distribution in the pore structure of the ferrierite catalysts is different when comparing coke deposited at 300°C and at 450°C. Most probably, a pore mouth plugging mechanism prevails at low temperature, which leads to a faster decrease in the available surface for reaction.

The reaction mechanism during the linear butene isomerization on FER still remains under discussion. On fresh FER, when the material is non-selective, it was proposed that the reaction occurs through either a bimolecular mechanism [18, 30] or a monomolecular one [13, 31] being the by-products formed on different active sites [31]. Evidences that a

substantial amount of isobutene is formed via the non-selective bimolecular mechanism simultaneously with the by-products were also reported [32]. On aged FER, when the material became selective, it is proposed that the bimolecular mechanism cannot occur, and that the monomolecular one takes place instead [18, 31, 33]. A pseudo-monomolecular mechanism was also reported in order to explain the FER's catalytic behavior [34]. By-product formation, mainly propene, pentenes and octenes as well as isobutene production initially take place via oligomerization and cracking throughout the FER crystals [20]. According to our by-product distributions, the very low amount of C_1 and C_2 fractions demonstrate that dimerization reaction takes place. The detailed analysis of the C_5^+ fraction show the presence of C_5, C_6 and C_7 products, mainly the corresponding alkenes, what further supports the oligomerization-cracking reactions path. The presence of butane among the by-products can be explained considering that hydrogen transfer reactions between coke precursors and linear butene molecules take place. These reactions were considered in the reaction scheme for the formation of carbonaceous deposits starting from butene [20]. Finally, at long TOS, when the carbonaceous deposit was already formed modifying the active sites and/or their environment, our results suggest the bimolecular mechanism still takes place and explains the by-product distribution.

4.2. Coke characterization

The larger amount of carbonaceous deposit on H-FER is formed during the first 30 min on stream [24]. There is a rapid coke formation on the fresh catalyst. Thereafter, the coke affects not only the desired reaction, but also the speed of coke deposition. The carbon content reaches levels between 7 and 9% [2, 13, 16-18]. These high carbon contents have been associated to the strong acid sites present on the catalyst surface [25]. According to our results, neither the W or B species impregnated on NH4-FER and the W

species exchanged on NH4-FER and K-FER nor the reaction temperature change the total amount of carbonaceous deposit formed on these samples. Then, it can be related to the strong acid sites present on these materials that leads to the high initial activity, also favoring the carbonaceous deposit formation. Nevertheless, the amount of coke deposited on B/FER is lower (4.5%) and significantly lower on W/K-FER (below 1.5%, independent of reaction temperature). The impregnation of B poisoned strong acid sites while W/K-FER has not these acid sites; it favors the desorption of products before the adsorption of reactants and/or reaction intermediates and their transformation into coke. Acid strength of active sites has a strong influence over the amount of the carbonaceous deposit formed during the butene reaction.

Both reaction temperature and type of active sites present on the catalyst surface have a strong influence on the temperature of combustion of each type of coke (different peaks) and their proportions, as indicated by the TPO profiles. The lower the reaction temperature, the lower the temperature at which the coke deposit starts combustion. It could be associated to differences in both coke composition and coke location. The low temperature peak is more hydrogenated, as previously reported [19], and therefore is more easily eliminated from the catalyst. Heating under an inert gas flow or under vacuum can even desorb this fraction. On the other hand, the first peak is also associated with coke located closer to the pore mouths, and therefore the kinetics for gasification will be faster.

After reaction at 300°C, the FTIR characterization of H-FER, W/FER, W-FER, W-K-FER, and B-FER shows the main bands corresponding to olefinic species (bands at 1390, 1420 and 1630 cm^{-1}) and to aromatic rings (band at 1512 cm^{-1}). The 1514 cm^{-1} band, corresponding to carbon-carbon bond vibration of hydrogen-rich non-condensed aromatics, was reported as the main band on deposits formed on H-FER after 4 h of operation [35, 36]. An aromatic nature of the coke formed during the linear butene skeletal

isomerization on FER was previously reported [2,30]. Nevertheless, Xu *et al.* [2] also reported the 1622 cm^{-1} band assigned to the stretching of butene double bond while Guisnet *et al.* [30] employed a different technique in order to remove and characterize the coke. Deposits formed on samples having strong acid sites also display the 1335 cm^{-1} band assigned to isobutene dimeric species. On W/K-FER having only weak acid sites, the 1512 cm^{-1} band is very weak, while bands at 1390 cm^{-1} (assigned to linear butenes) and at 1628 cm^{-1} (assigned to isobutene π-bond and/or olefinic species) increase. Then, coke formed on W/K-FER presents a larger olefinic nature, while the band corresponding to dimeric species is not detected. It allows us to consider the isobutene dimeric species play an important role in coke formation. The role of dimers in the scheme for the transformation of carbonaceous deposits starting from butene, was reported [20].

After reaction at 450°C, only the high-temperature combustion peak appears on all samples and the coke deposits display mainly an aromatic nature, which is characterized by the 1590 cm^{-1} band. These deposits need higher temperatures to be burnt-out. These results indicate that the reaction temperature has also a strong influence on the nature of coke. The higher the reaction temperature, the lower the amount of different type of combustion peaks displayed in the TPO profile. At higher reaction temperature, the amount of the aromatic coke is proportionally higher than the olefinic one, because a higher temperature favors the aromatization of oligomers, as previously shown [16].

CONCLUSIONS

The linear butene skeletal isomerization on ferrierite modified with W or B species was measured at 300 and 450°C. The following remarks can be made:

* W/FER, W-FER, W-K-FER, and B-FER, all catalysts having strong acid sites, display at 300°C and a short TOS practically the same high butene conversion with low isobutene selectivity. The presence of those acid sites favors undesirable side reactions diminishing the isobutene selectivity. Conversion decreases at long TOS. According to the sample, the isobutene yield shows different pattern. At a short TOS, W-K-FER produces the largest yield being two times the H-FER corresponding one. At long TOS, B-FER reaches the largest isobutene production, being larger than the previous reported to W-K-FER. At 450°C, samples show more stability, maintaining the high conversion even at long TOS. Independent of temperature, the carbonaceous deposit formed on these samples is large, between 6.0 and 7.4%.

* W/K-FER, sample without strong acid sites, is active in the isobutene production. Two main characteristics present this catalyst: the high isobutene yield at 450°C which is practically the same reached with W/FER, although its conversion is only a half of the W/FER one. The other characteristic is the smallest amount of carbonaceous deposit formed on this material, lower than 1.5%.

* B/FER presents an intermediate behavior. The incipient wet impregnation of boron on ferrierite diminishes both conversion and isobutene yield, being the carbon content between the previous ones.

* According to by-product distributions, dimerization and oligomerization reactions take place.

* The acid strength of active sites has a strong influence over the amount of carbonaceous deposit formed. Samples with strong acid sites form larger amount of coke. The reaction temperature and the type of acid sites have influence on the nature of the carbonaceous deposit formed. W/K-FER, without strong acid sites, after reaction at 300°C only displays the low-temperature combustion peak. Both olefinic species and aromatics rings are detected in the carbonaceous deposit formed during reaction at 300°C. At 450°C, the amount of the aromatic coke increases because a higher

temperature favors the aromatization of oligomers. Isobutene dimeric species play a role in coke formation.

ACKNOWLEDGMENTS

REFERENCES

1. Mooiweer, H. H., Suurd, J., and de Jong, K. P. 1993, European Patent 0 574 994 A1, to SHELL Internationale.
2. Xu, W. Q., Yin, Y. G., Suib, S. L., and O'Young, C. L. 1995, J. Phys. Chem., 99, 758.
3. Finelli, Z. R., Fígoli, N. S., and Comelli, R. A. 1998, Catal. Lett., 51, 223.
4. Finelli, Z. R., Querini, C. A., Fígoli, N., and Comelli, R. A. 2001, Appl. Catal. A, 216, 91.
5. O'Young, C. L., Xu, W. Q., Simon, M., and Suib, S. L. 1994, in: J. Weitkamp, H. Karge, H. Pfeifer, W. Hölderich (Eds.), Zeolites and Related Microporous Materials: State of the Art, Studies in Surface Science and Catalysis, vol. 84, Elsevier, Amsterdam, p. 1671.
6. Datka, J., and Piwowarska, Z. 1989, J. Chem. Soc., Faraday Trans. I, 85(1), 47.
7. Attfield, M. P., Weigel, S. J., and Cheetham, A. K. 1997, J. Catal., 172, 274.
8. Dalconi, M. C., Cruciani, G., Alberti, A., Ciambelli, P., and Rapacciuolo, M. T. 2000, Microporous and Mesoporous Mat., 39, 423.
9. Mériaudeau, P., Tuan, V. A., Hung, L. N., Naccache, C., and Szabo, G. 1997, J. Catal., 171, 329.
10. Cañizares, P., and Carrero, A. 2000, Catal. Lett., 64, 239.
11. Komatsu, T., Ishihara, H., Fukui, Y., and Yashima, T. 2001, Appl. Catal. A, 214, 103.
12. Guisnet, M., and Magnoux, P. 1997, Catal. Today, 36, 477.
13. Seo, G., Jeong, H. S., Jang, D. L., Cho, D., and Hong, S. B. 1996, Catal. Lett., 41, 189.
14. Xu, W. Q., Yin, Y. G., Suib, S. L., Edwards, J. C., and O'Young, C. L. 1995, J. Phys. Chem., 99, 9443.
15. Seo, G., Kim, N. H., Lee, Y. H., and Kim, J. H. 1999, Catal. Lett., 57, 209.
16. Comelli, R. A., Finelli, Z. R., Fígoli, N., and Querini, C. A. 1997, in: C.H. Bartholomew, G. Fuentes (Eds.), Catalyst Deactivation 1997, Studies in Surface Science and Catalysis, vol. 111, Elsevier, Amsterdam, p. 139.
17. Guisnet, M., Andy, P., Boucheffa, Y., Gnep, N. S., Travers, C., and Benazzi, E. 1998, Catal. Lett., 50, 159.
18. de Jong, K. P., Mooiweer, H. H., Buglass, J. G., Maarsen, P. K. 1997, in: C.H. Bartholomew, G. A. Fuentes (Eds.), Catalyst Deactivation 1997, Studies in Surface Science and Catalysis, vol. 111, Elsevier, Amsterdam, p. 127.
19. Finelli, Z. R., Querini, C. A., Fígoli, N., and Comelli, R. A. 1999, Appl. Catal. A, 187, 115.
20. van Donk, S., Bitter, J. H., and de Jong, K. P. 2001, Appl. Catal., A, 212, 97.
21. Comelli, R. A. 2002, Catal. Lett., 83, 257.
22. Fung, S. C., and Querini, C. A. 1992, J. Catal., 138, 240.
23. Datka, J., and Piwowarska, Z. 1989, J. Chem. Soc., Faraday Trans., I, 85(4), 837.
24. Brascó, G. N., and Comelli, R. A. 2001, Catal. Lett., 71, 111.
25. Finelli, Z. R., Querini, C. A., and Comelli, R. A. 2003, Appl. Catal., A, 247, 143.
26. Wichterlová, B., Zilkova, N., Uvarova, E., Cejka, J., Sarv, P., Paganini, C., and Lercher, J. A. 1999, Appl. Catal. A ,182, 297.
27. Xu, W. Q., Yin, Y. G., Suib, S. L., Edwards, J. C., and O'Young, C. L. 1996, J. Catal., 163, 232.
28. Kwak, B. S., and Sung, J. 1998, Catal. Lett., 53, 125.

29. Baeck, S. H., and Lee, W. Y. 1997, Appl. Catal. A, 164, 291.

30. Guisnet, M., Andy, P., Gnep, N. S., Travers, C., and Benazzi, E. 1997, in: H. Chon, S. K. Ihm, Y. S. Uh (Eds.), Progress in Zeolite and Microporous Materials, Studies in Surface Science and Catalysis, vol. 105, Elsevier, Amsterdam, p. 1365.

31. Houzvicka, J., and Ponec, V. 1997, Ind. Eng. Chem. Res., 36, 1424.

32. Cejka, J., Wichterlová, B., and Sarv, P. 1999, Appl. Catal. A, 179, 217.

33. Mériaudeau, P., Bacaud, R., Ngoc Hung, L., and Vu, A. T. 1996, J. Mol. Catal. A, 110, L177.

34. Andy, P., Gnep, N. S., Guisnet, M., Benazzi, E., and Travers, C. 1998, J. Catal., 173, 322.

35. van Donk, S., Bus, E., Broersma, A., Bitter, J. H., and de Jong, K. P. 2002, J. Catal., 212, 86.

36. van Donk, S., Bus, E., Broersma, A., Bitter, J. H., and de Jong, K. P. 2002, Appl. Catal. A, 237, 149.